

Interactive slice visualization for exploring machine learning models

Catherine B. Hurley, Mark O’Connell, Katarina Domijan

Department of Mathematics and Statistics, Maynooth University

October 11, 2021

Abstract

Machine learning models fit complex algorithms to arbitrarily large datasets. These algorithms are well-known to be high on performance and low on interpretability. We use interactive visualization of slices of predictor space to address the interpretability deficit; in effect opening up the black-box of machine learning algorithms, for the purpose of interrogating, explaining, validating and comparing model fits. Slices are specified directly through interaction, or using various touring algorithms designed to visit high-occupancy sections or regions where the model fits have interesting properties. The methods presented here are implemented in the R package **condvis2**.

Keywords: Black-Box Models; Supervised and Unsupervised learning; Model explanation; XAI; Sectioning; Conditioning

1 Introduction

Machine learning models fit complex algorithms to extract predictions from datasets. Numerical model summaries such as mean squared residuals and feature importance measures are commonly used for assessing model performance, feature importance and for comparing various fits. visualization is a powerful way of drilling down, going beyond numerical summaries to explore how predictors impact on the fit, assess goodness of fit and compare multiple fits in different regions of predictor space, and perhaps ultimately developing improved fits. Coupled with interaction, visualization becomes an even more powerful model exploratory tool.

Currently, explainable artificial intelligence (XAI) is a very active research topic, with the goal of making models understandable to humans. There have been many efforts to use visualization to understand machine learning fits in a model-agnostic way. Many of these show how features locally explain a fit (Ribeiro et al., 2016; Lundberg and Lee, 2017). Staniak and Biecek (2018) give an overview of R packages for local explanations and present some nice visualizations. Other visualizations such as partial dependence plots (Friedman, 2001) shows how a predictor effects the fit on average. Drilling down, more detail is obtained by exploring the affect of a designated predictor on the fit, conditioning on fixed values of other predictors, for example using the individual conditional expectation (ICE) curves of Goldstein et al. (2015). Interactive visualizations are perhaps underused in this context. Baniecki and Biecek (2020) offer a recent discussion. Britton (2019) uses small multiple displays of clustered ICE curves in an interactive framework to visualize interaction effects.

In this paper, all visualizations are based on slicing high-dimensional space, where interaction is used to navigate the slices through the space. The idea of using interactive visualization in this way was introduced in O’Connell et al. (2017). The basic concept is to fix the values of all but one or two predictors, and to display the conditional fitted curve or surface. Observations from a slice around the fixed predictors are overlaid on the curve or surface. The resulting visualizations will show how predictors affect the fitted model and the model goodness of fit, and how this varies as the slice is navigated through predictor

space.

Visualising data via conditioning was popularised by the “small multiples” of Tufte (Tufte, 1986) and the trellis displays of Becker et al. (1996). Nowadays, the concept is widely known as *facetting*, courtesy of Wickham (2016). Wilkinson (2005) (chapter 11) gives a comprehensive description. In the context of machine learning models, the conditioning concept is used in ICE plots (Goldstein et al., 2015), which show a family of curves giving the fitted response for one predictors, fixing other predictors at observed values. These ICE plots simultaneously show all observations and overlaid fitted curves, one for each observation in the dataset. Partial dependence plots (Friedman, 2001) which show the average of the ice curves are more popular but these are known to suffer from bias in the presence of correlated predictors. The recent paper of (Hurley, 2020) gives a comparison of these and other model visualization techniques based on conditioning.

In O’Connell et al. (2017) and its R package implementation **condvis** (O’Connell et al., 2016) we described how conditional visualization is used to interactively explore model fits. The package **condvis** used the platform of base R graphics and interaction primarily, which is an interesting use-case, but the platform lacks a toolkit of menus and sliders which limited the interactivity of our application.

In the current paper we extend conditional visualization to a far broader sweep of machine learning techniques including density estimation and clustering. We also describe touring algorithms for exploring predictor space. These algorithms make conditional visualization a practical and valuable tool for model exploration as dimensions increase. All the methods described here are implemented in a more recent package called **condvis2** (Hurley et al., 2019), which uses the Shiny platform (Chang et al., 2020) to provide a highly-interactive application for model exploration.

We review the basic ideas of conditional visualization for model fits in Section 2, following O’Connell et al. (2017). We describe the embedding of these visualizations in an interactive Shiny application (**condvis2**) in Section 3. In Section 4 we describe how the design of **condvis2** means that our visualizations are available for most model-fitting algorithms available in R. We also present extensions to unsupervised learning problems and

for visualising density estimates. As the dimension of the conditioning space increases, constructing useful and informative slices is more challenging. In Section 5 we investigate the limitations of conditional visualization in this setting. Our proposal here is to find *interesting* slices, thus constructing automatic *tours* of the conditioning space. In Section 6 we present case studies, illustrating how our methods are used to understand predictor effects, explore lack of fit and to compare multiple fits. Finally we conclude with a discussion.

2 Conditional visualization for model fits

Consider data $\{\mathbf{x}_i, y_i\}_{i=1}^n$, where $\mathbf{x}_i = (x_{i,1}, \dots, x_{i,p})$ is a vector of predictors and y_i is the response. Let \hat{f} denote a fitted model that maps the predictors \mathbf{x} to fitted responses $\hat{f}(\mathbf{x})$. Let $S \subset \{1, \dots, p\}$ index the *section predictor(s)* and its the complement set $C = \{1, \dots, p\} \setminus S$ the *conditioning predictor(s)*. Corresponding to S and C , partition the feature coordinates \mathbf{x} into \mathbf{x}_S and \mathbf{x}_C . Similarly, let $\mathbf{x}_{i,S}$ and $\mathbf{x}_{i,C}$ denote the coordinates of observation i for the predictors in S and C respectively. We have interest in observing the relationship between the response y and \hat{f} and \mathbf{x}_S , conditional on \mathbf{x}_C . For our purposes, a section or slice is constructed as a region around a single point in the space of C , i.e. $\mathbf{x}_C = \mathbf{u}_C$, where \mathbf{u}_C is called the *section point*.

2.1 Section plots

A *section plot* consists of a display of $\hat{f}(\mathbf{x}_S = \mathbf{x}_S^g, \mathbf{x}_C = \mathbf{u}_C)$ versus \mathbf{x}_S^g , overlaid on a subset of observations $(\mathbf{x}_{i,S}, y_i)$, where $\mathbf{x}_{i,C}$ is near the designated section point \mathbf{u}_C . Here \mathbf{x}_S^g denotes a grid covering the predictors \mathbf{x}_S . For displaying model fits, we use $|S| = 1, 2$.

The section plot displays used in **condvis2** depend on the prediction (numerical, factor, or probability matrix) and predictor type (numerical or factor). Figure 1 shows different section plots. For two numeric section variables, we also use perspective displays. When section predictors are factors these are converted to numeric, so the displays are similar to those shown in the rows and columns labelled n/f. When the prediction is the probability of factor level, the display uses a curve for one of the two levels as in Figure 1(b) and

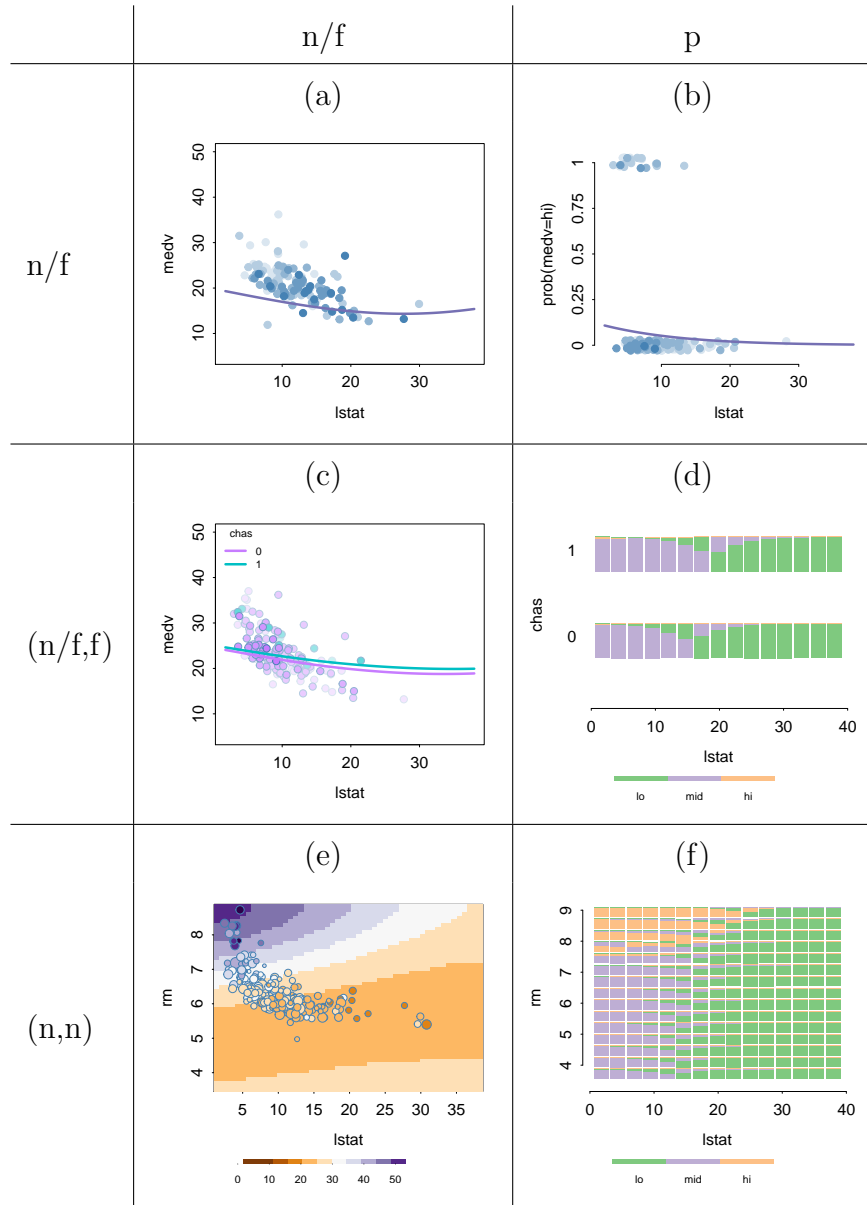


Figure 1: Section plot displays. The column label represents the prediction n =numerical, f =factor, p =probability of factor level. The row label represents the type of one or two section variables. Factor predictions and section variables are converted to numeric, so those displays are similar to those from numeric. When the prediction is probability of factor level, the display uses curves for two levels and bars otherwise.

barplot arrays otherwise, see Figure 1(d) and (f). Here the bars show the predicted class probabilities, for levels of a categorical section variable, and bins of a numeric section variable. (The display choices we provide in **condvis2** are a modified and expanded version of those in package **condvis**, shown as Figure 10 in O’Connell et al. (2017)).

For each observation, $i = 1, 2, \dots, n$, we compute how far it is from the section point \mathbf{u}_C using

$$d_i = d(\mathbf{u}_C, \mathbf{x}_{i,C}) \quad (1)$$

where d is a distance measure. This distance is converted to a similarity score as

$$s_i = \max\left(0, 1 - \frac{d_i}{\sigma}\right) \quad (2)$$

where $\sigma > 0$ is a threshold parameter set by the user. Distances exceeding the threshold σ are accorded a similarity score of zero. Points on the section, that is, identical to the section point \mathbf{u}_C , receive the maximum similarity of 1. Plotting colours for points are then faded to the background white colour using these similarity scores. Points with a similarity score of zero become white, that is, are not shown. Non-zero similarities are binned into (by default five) equal-width intervals. The colours of observations whose similarity belongs to the right-most interval are left unchanged. Other observations are faded to white, with the amount of fade decreasing from the first interval to the last. See for example the fading colours in Figure 1(a), (b), (c).

For section plot displays such as Figure 1(e) where fit \hat{f} is shown as an image, faded points would be hard to see, so instead we shrink the overlaid observations in proportion to the similarity score. There is as yet no layer of observations added to the barplot arrays in Figure 1(d) and (f), but we suspect this may overload the plots.

We use two different notions of “distance” in **condvis2**. The first is a Minkowski distance between numeric coordinates (Equation 3). For two vectors \mathbf{u} and \mathbf{v} , where C_{num} indexes numeric predictors and its complement C_{cat} indexes the categorical predictors in the conditioning set C ,

$$d_M(\mathbf{u}, \mathbf{v}) = \begin{cases} \left(\sum_{j \in C_{num}} |\mathbf{u}_j - \mathbf{v}_j|^q\right)^{1/q} & \text{if } \mathbf{u}_k = \mathbf{v}_k \ \forall k \in C_{cat} \\ \infty & \text{otherwise.} \end{cases} \quad (3)$$

Currently, we use Euclidean distance given by $q = 2$ and the maxnorm distance which is the limit as $q \rightarrow \infty$ (equivalently $\max_j |u_j - v_j|$). With the Minkowski distance, points whose categorical coordinates do not match those of the section \mathbf{u}_C exactly will receive a similarity of zero and will not be visible in the section plots. Using Euclidean distance, visible observations in the section plot will be in the hypersphere of radius σ centred at \mathbf{u}_C . Switching to the maxnorm distance means that visible observations will be in the unit hypercube with sides of length 2σ .

If there are many categorical conditioning predictors, requiring an exact match on categorical predictors could mean that there are no visible observations. For this situation, we include a Gower distance (Gower, 1971) given in Equation 4 which combines absolute differences in numeric coordinates and mismatch counts in categorical coordinates,

$$d_G(\mathbf{u}, \mathbf{v}) = \sum_{k \in C_{num}} \frac{|u_k - v_k|}{R_k} + \sum_{k \in C_{cat}} 1[u_k \neq v_k] \quad (4)$$

where R_k is the range of the k th predictor in C_{num} .

Figure 2 provides an illustration in the simple setting with just two predictors. Figure

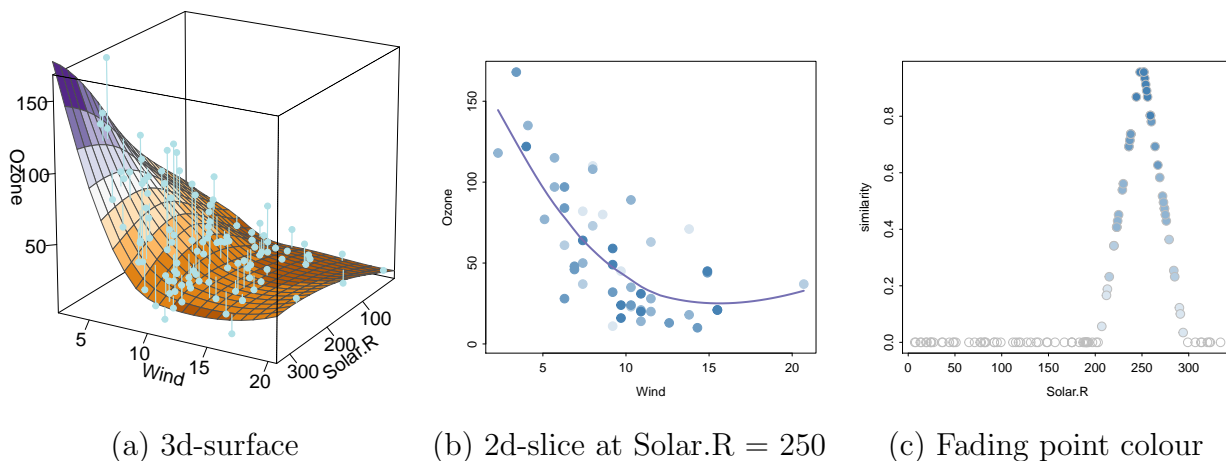


Figure 2: visualization of Ozone loess fit as a surface in (a), as a curve versus Wind conditioning on Solar.R=250 in (b). Panel (c) shows in blue how point colours are faded as distance to Solar.R=250 increases and similarity decreases. The grey circles have a similarity score of zero and are not visible in panel (b).

2(a) shows a loess surface relating Ozone to Solar.R and Wind in the airquality data

(Chambers et al., 1983). Figure 2(b) shows how the surface varies with Wind, with Solar.R fixed at 250. Only observations with Solar.R near 250 (here about 250 ± 50) are shown. Observations in this window receive a similarity score related to their distance from 250, which is used to fade the colour by distance. Observations outside the window receive a similarity score of zero and are not displayed in Figure 2(b). In (c), the similarity scores assigned to observations using their distance to Solar.R=250 are plotted, non-zero similarity scores are faded by decreasing similarity. By decreasing the Solar.R value (interactively or otherwise) we see that the dependence of Ozone on Wind also decreases. Figure 3 shows the conditional visualization of the loess curve at Solar.R =150 and 50. It is also

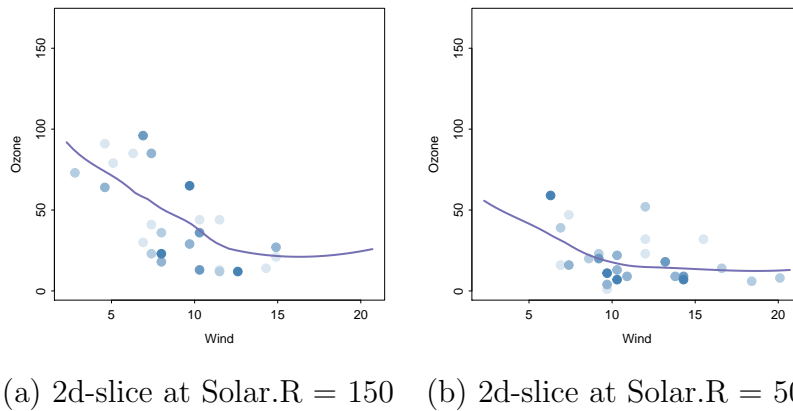


Figure 3: Conditional visualization of Ozone loess surface versus Wind, fixing Solar.R

apparent in (b) that for Solar.R = 50 there are no observations with Wind below 6, so Ozone predictions for low Solar.R and Wind are extrapolations.

2.2 Condition selector plots

Plots are made of the predictors in the conditioning set C . Either predictors are plotted singly or in pairs using scatterplots, histograms, boxplots or barplots as appropriate. These are the *condition selector plots*. They show the distributions of conditioning predictors and also serve as an input vehicle for new settings of these predictors. A pink cross overlaid on the condition selector plots shows the current settings of the section point \mathbf{u}_C , which is under interactive control. We use the strategy presented in O’Connell et al. (2017) for ordering conditioning predictors to avoid unwitting extrapolation.

Alternatively, predictors may be plotted using a parallel coordinates display. It is more natural in this setting to restrict conditioning values to observations. In this case, the current settings of the section point \mathbf{u}_C are shown as a highlighted observation. In principle a scatterplot matrix could also be used, but we do not provide for this option as it uses too much screen real estate.

3 Interactive exploration with `condvis2`

visualization along with interactivity is a natural and powerful way of exploring data; so-called *brushing* (Stuetzle, 1987) is probably the best-known example. Other data visualization applications have used interaction in creative ways, for high-dimensional data `ggobi` (see for example Cook and Swayne (2007)) offers various kinds of low-dimensional dynamic projection tours while the recent R package `loon` (Waddell and Oldford, 2020) offers a graph-based interface for moving through series of scatterplots. The interactive display paradigm has also been applied to exploratory modelling analysis, for example Urbanek (2002) describes an application for exploratory analysis of trees.

In the R environment, there are a number of platforms for building interactive applications. The most primitive of these is base R with its function `getGraphicsEvent` which offers control of mouse and keyboard clicks, used by our previous package `condvis` (O’Connell et al., 2016; O’Connell, 2017), but the lack of support for other input mechanisms such as menus and sliders limits the range of interactivity. The package `loon` uses `tcltk` for interactivity. For `condvis2` we have chosen to use Shiny which is relatively easy to use, provides a browser-based interface and supports web-based sharing. We use visualizations from base R graphics, rather than `ggplot2` (Wickham, 2016) for reasons of speed.

3.1 The `condvis2` layout

We introduce a dataset here which we will visit again in Section 6. The bike sharing dataset `bike` (Fanaee-T and Gama, 2013) available from the UCI Machine Learning Repository has

a response which is the count of rental bikes (`nrentals`) and the goal is to relate this to weather and seasonal information, through features which are `season`, `hol` (holiday or not), `wday` (working day or not), `yr` (year 2011 or 2012), `weather` (good, misty, bad), `temp` (degrees Celcius), `hum` (relative humidity in percent) and `wind` (speed in km per hour). The aim is to model the count of rental bikes between years 2011 and 2012 in a bike share system from the corresponding weather and seasonal information. We build a random forest (Breiman, 2001) fit called `mod.rf` relating `nrentals` to other features for all 750 observations, and set up a **condvis2** application with

```
condvis(bike, model= mod.rf, response="nrentals", sectionvars="temp")
```

Our application supports a broad range of machine learning fits (discussed in Section 4.1) which could be used in place of the random forest in this example. Here dataset variables other than `nrentals` and `temp` become the condition variables, though the condition variables may also be specified as another input to `condvis`. This code opens up a browser with a display as in Figure 4.

If the initial value of the conditioning predictors is not specified in the call to `condvis`, this is set to the medoid of all predictors, calculated using standardised Euclidean distance, or Gower for predictors of mixed type. Here the medoid is represented by the pink crosses in the condition selector plots on the right hand panel, and these values are also listed underneath as `hum=58.0`, `wind=11.8`, `season=sum`, `weather=good`, `wday=y`, `hol=n`, `yr=2011`. The plot of `nrentals` versus `temp` on the left hand side shows the random forest fit as `temp` varies, for fixed values of the conditioning predictors. As the distance measure used defaults to `maxnorm`, the observations appearing on this plot all have `season=sum`, `weather=good`, `wday=y`, `hol=n`, `yr=2011`, and have `wind` and `hum` values within one (the default value of σ in Equation 2) standard deviation of `hum=58.0`, `wind=11.8`. The point colours are faded as the `maxnorm` distance from (`hum=58.0`, `wind=11.8`) increases. These observations also appear with a black outline on the (`hum`, `wind`) condition selector plot.

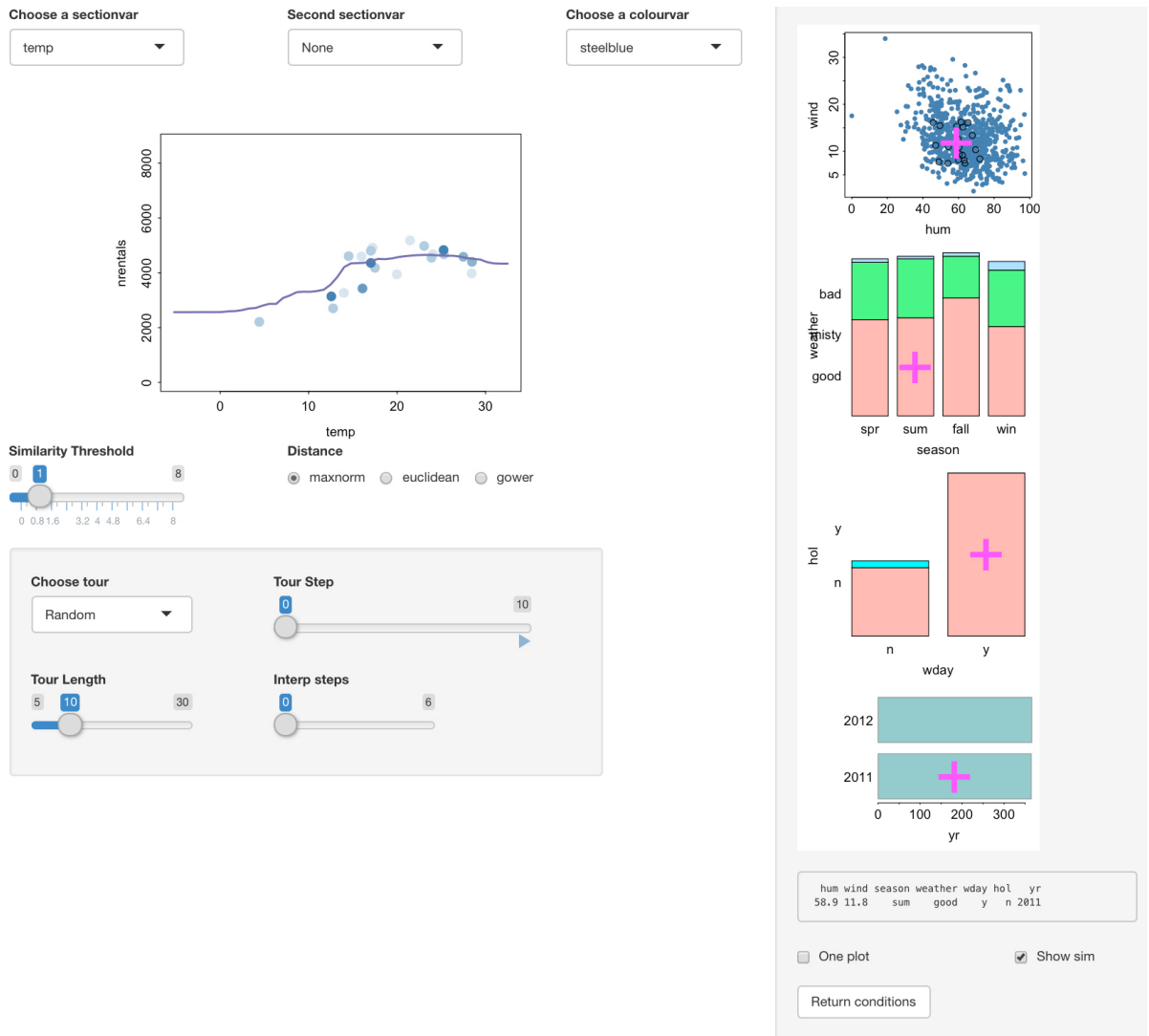


Figure 4: Condis2 screenshot for a random forest fit to the bike rentals data.

3.2 Interaction with condvis2

The choice of the section point \mathbf{u}_C is under interactive control. For example clicking on the (hum, wind) plot in Figure 4 will move the coordinates of \mathbf{u}_C for these two variables to the new location, while the values for other predictors in C are left unchanged. This is the main way of driving exploration of fits while moving through slices of conditioning space. This form of selection is similar to brushing with multi-dimensional brushes as described in Martin and Ward (1995). The light grey panel on the lower left offers another way of navigating slices of predictor space, other than interacting with the condition selector plots. This functionality will be discussed in Section 5.

Clicking on the similarity threshold slider increases or decreases the value of σ , including more or less observations in the nrentals versus temp plot. The distance used for calculating similarities may be changed from maxnorm to Euclidean or Gower (see Equations 3 and 4) via the radio buttons. When the threshold slider is moved to the right-most position, all observations are included in the section plot display. All of the plots in the condition selector panel on the right are interactive. Clicking on a new location in the (hum, wind) plot, say hum=90, wind=10, moves the pink cross, but the pink crosses in the other plots do not change. Immediately the section plot of nrentals versus temp shows the random forest fit at the newly specified location, but now there is only one observation barely visible in the section plot, telling us that the current combination of the conditioning predictors is in a near-empty slice. It is also possible to click on an observation in the section plot, and this has the effect of moving the section point \mathbf{u}_C to the coordinates of the selected observation for the conditioning predictors.

One or two section variables may be selected from the “Choose a sectionvar” and “Second sectionvar” menus. If the second section variable is hum, say, this variable is removed from the condition selector plots. With two numeric section variables, the section plot appears as an image as in Figure 1(e). Another checkbox “Show 3d surface” appears, and clicking this shows how the fit relates to (temp, hum) as a rotatable 3d plot. Furthermore, a variable used to colour observations may be chosen from the “Choose a colourvar” menu.

Clicking the “One plot” checkbox on the lower right changes the condition selector

plots to a single parallel coordinate plot. Deselecting the “Show sim” box causes the black outline on the observations in the current slice to be removed, which is a useful option if the dataset is large and display speed is an issue. Clicking on the “Return conditions” button causes the app to exit, returning all section points visited as a data frame.

4 Machine learning: supervised, unsupervised and density estimation

In this section we describe how the design of **condvis2** means that our visualizations are available for most model-fitting algorithms available in R. One can also think of clustering and density estimation algorithms as providing a “fit”, and we discuss how our methods provide visualizations in these settings.

4.1 Which fits?

visualizations in **condvis2** are constructed in a model-agnostic way. In principle all that is required is that a fit produces predictions. Readers familiar with R will know that algorithms from random forest to logistic regression to support vector machines all have some form of `predict` method, but they have different arguments and interfaces.

We have solved this by writing a predict wrapper called `CVpredict` (for `condvis predict`) that operates in a consistent way for a wide range of fits. Here is the generic function for `CVpredict` :

```
CVpredict <- function(fit, newdata, ..., ptype = "pred", pthreshold = NULL,
                     ylevels = NULL, ptrans = NULL, pinterval = NULL,
                     pinterval_level = 0.95) {
  UseMethod("CVpredict", fit)
}
```

- `fit` is the fitted model

- `newdata` is a `data.frame` from which predictions are to be obtained. No special order is needed for the variables in `newdata`.
- `ptype` refers to the type of prediction. The default, `pred`, yields numeric predictions for regression and factors for classification. Other possibilities appropriate for classification models are `prob`, which gives a probability for the last class, or `probmatrix` which gives a matrix where columns correspond to the factor levels. `pthreshold` is used in the two-class case to threshold probabilities to arrive at a factor. `ptrans` is for functions such as `log` that might be provided to the numeric prediction.
- `ylevels` is an optional parameter specifying the response factor levels, helpful to get consistency across the levels of the response factor.
- `pinterval` takes values `confidence` or `prediction` or `NULL` and `pinterval_level` is the interval level.
- `...` is for other arguments to individual predict methods.

We provide over 30 `CVpredict` methods, for fits ranging from neural nets, to trees to bart machine. And, it should be relatively straightforward for others to write their own `CVpredict` method, using the template we provide.

Others have tackled the problem of providing a standard interface to the model fitting and prediction tasks. The `parsnip` package (Kuhn and Vaughan, 2019) part of the so-called tidyverse world streamlines the process and currently includes drivers for about 40 supervised learners including those offered by `spark` and `stan`. The packages `caret` (Kuhn, 2019), `mlr` (Bischl et al., 2016), and its most recent incarnation `mlr3` interface with hundreds of learners and also support parameter tuning. As part of `condvis2`, we have written `CVpredict` methods for the model fit classes from `parsnip`, `mlr`, `mlr3` and `caret`. Therefore our `condvis2` visualizations are accessible from fits produced by most of R’s machine learning algorithms.

4.2 Clustering

Typical ways to display clustering results include assigning colours to observations reflecting cluster membership, and visualising the coloured observations in a scatterplot matrix, parallel coordinate plot or in a plot of the first two principal components. Some clustering algorithms

such as k-means and model-based clustering algorithms offer predictions for arbitrary points. The results of such algorithms can be visualized with **condvis2**.

For the well-known Swiss banknote data recording the dimensions of 200 counterfeit and genuine Swiss notes (Flury, 1988) Figure 5 shows the results of a 3-cluster k-means fit to the variables

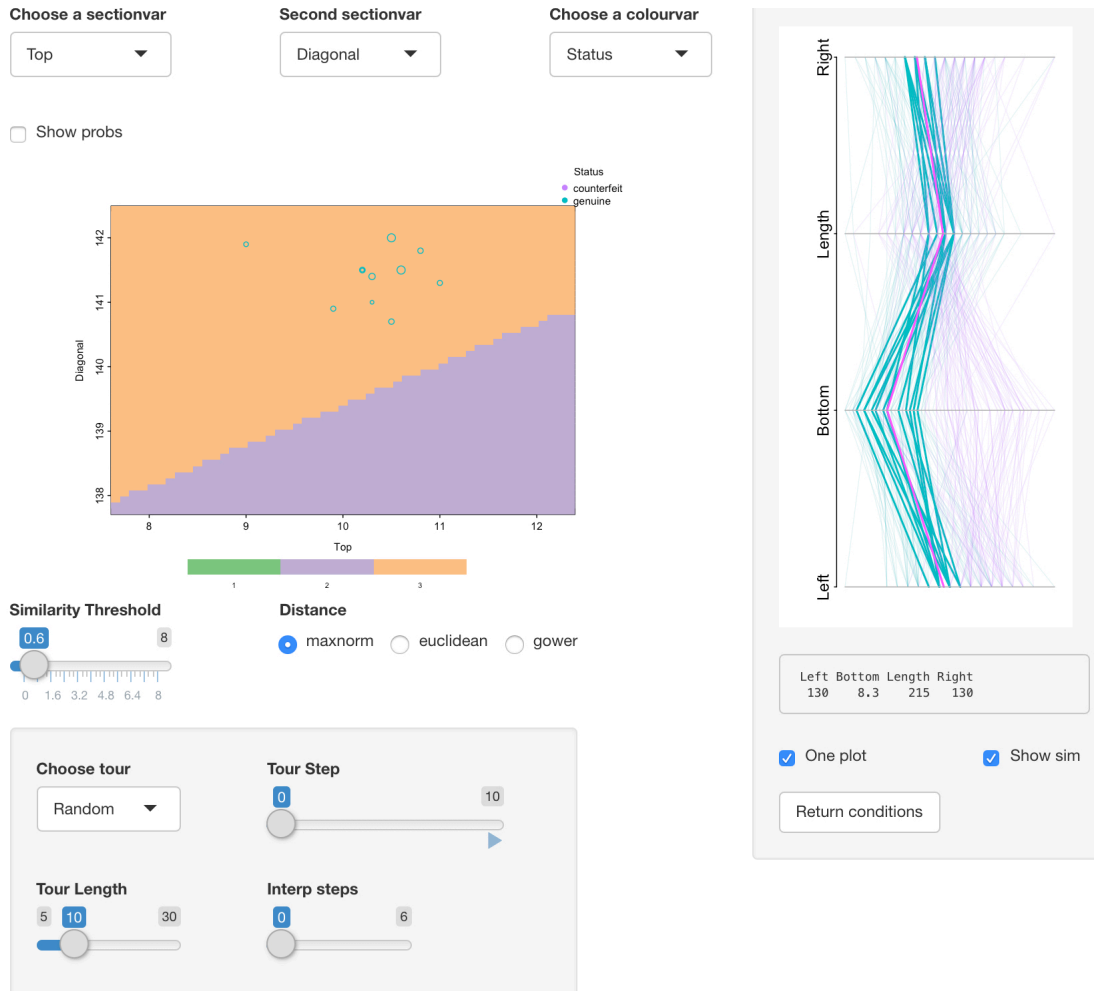


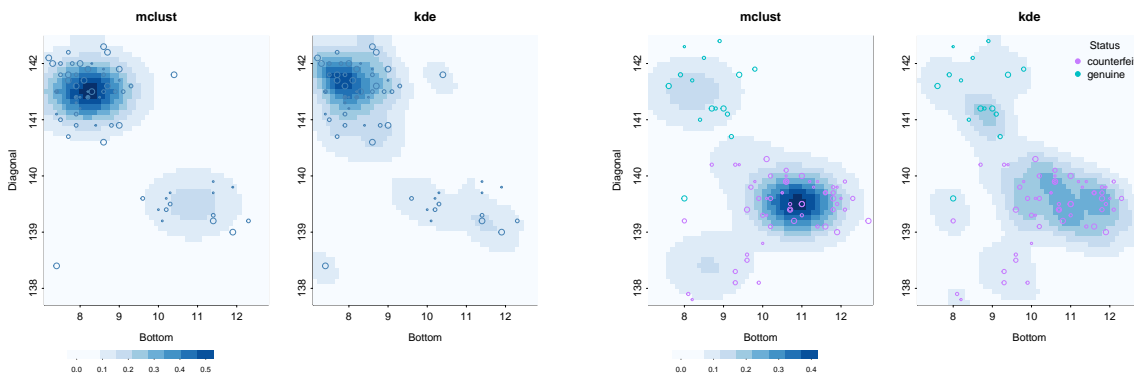
Figure 5: K-means fit with three clusters of Swiss Banknote data, conditioning on centroid for genuine notes

Length, Left, Right, Bottom, Top and Diagonal. The section predictors are Top, Diagonal and the remaining predictors are conditioning predictors displayed as a parallel coordinate plot. Conditioning on the centroid of the genuine notes, we see that k-means divides the Top-Diagonal plot between cluster 2 and cluster 3. All visible points belong to genuine notes, as they have a green outline. The clustering algorithm assigns these points to cluster 3, as the interior is orange. If we

condition instead on the centroid of the counterfeit notes the visible points are split between the other two clusters (not shown).

4.3 Density functions as fits

Density functions may also be explored with `condvis2`. For density fits, the `CVpredict` function gives the density value, which is renormalised over the section plot to integrate to 1. This way section plots show the density conditional on the settings of the conditional variable. As an example, we used model-based clustering using `mclust` (Scrucca et al., 2016) and a kernel density to estimate the density of Right, Bottom and Diagonal from the Banknote data. The `mclust` algorithm picks a mixture of four Gaussians where each component has the same covariance matrix. Figure 6 compares the `mclust` and `kde` estimates for the joint density of Bottom and



(a) Right at lower quartile

(b) Right at upper quartile

Figure 6: Density estimates (`mclust` and `kde`) of Diagonal, Bottom, Right of Swiss Banknote data, conditioning on levels of Right.

Diagonal conditional on Right. The two algorithms give similar joint densities for Right at the lower quartile (Figure 6(a)), but the more flexible nature of the kernel density estimate is apparent at the higher value of Right (Figure 6(b)).

5 Touring predictor space

We discuss challenges posed by dataset size and present algorithms for touring predictor space.

5.1 Dataset size

visualization of large datasets is challenging, particularly so in interactive settings where a user expects near-instant response. We have used **condvis2** in settings with $n = 100,000$ and $p = 30$ and the computational burden is manageable.

For section displays, the number of points displayed is controlled by the similarity threshold σ and is usually far below the dataset size n . For reasons of efficiency, condition selector displays by default show at most 1,000 observations, randomly selected in the case where $n > 1000$. Calculation of the medoid for the initial section point and the `kmedPath` (see Section 5.3.1) requires calculation of a distance matrix which has complexity $O(n^2p)$. For interactive use speed is more important than accuracy so we base these calculations on a maximum of 4,000 rows by default.

The conditioning displays show $\lceil p/2 \rceil$ panels of one or two predictors or one parallel coordinate display. Up to $p = 30$ will fit on screen space using the parallel coordinate display, perhaps 10-15 otherwise. Of course many data sets have much larger feature sets. In this situation, we recommend selecting a subset of features which are *important* for prediction, to be used as the section and conditioning predictors S and C . The remaining set of predictors, say F , are hidden from view in the condition selector plots and are fixed at some initial value which does not change throughout the `condvis` exploration. The initial predictor setting is under user control, and defaults to the medoid of the predictors.

Note that though the predictors F are ignored in the calculation of distances in Equations 3 and 4 and thus in the similarity scores of Equation 2, the initial values of these predictors $\mathbf{x}_F = \mathbf{u}_F$ are used throughout in constructing predictions; thus the section plot shows $\hat{f}(\mathbf{x}_S = \mathbf{x}_S^g, \mathbf{x}_C = \mathbf{u}_C, \mathbf{x}_F = \mathbf{u}_F)$. If the set of important predictors is not carefully selected, the fit displayed will not be representative of the fit for all observations visible in the section plot.

Another limitation of the methods of Section 3 is that exploring sections through interaction with condition selector plots becomes infeasible for $p > 6$. Our proposed automatic touring algorithms of Section 5.3 should help address this.

5.2 High dimension conditioning space

The *curse of dimensionality* Bellman (1961) refers to the sparseness of data in high dimensions. This implies that as the dimension of the conditioning space increases, conditioning on predictor

settings will yield empty sections. Scott (2015) (section 1.5) and Hastie et al. (2009) (section 2.5) both give excellent discussions of the consequences of this sparseness.

We will do some calculations to see how sparseness affects the number of visible observations in sections plots, for theoretical settings: For p independent $\text{Normal}(0,1)$ variables, the probability an observation is within 1 of the origin on all dimensions is $(\Phi(1) - \Phi(-1))^p$, where Φ is the cumulative density function of the standard Normal distribution. For independent $\text{Uniform}(-\sqrt{3}, \sqrt{3})$ variables the probability is $(1/\sqrt{3})^p$. (We use a range of $(-\sqrt{3}, \sqrt{3})$ for the Uniform corresponding to a standard deviation of 1, for comparison with $\text{Normal}(0,1)$.) Table 1 shows the expected

Table 1: The expected number of observations out of 2,000 to be within a threshold of 1 of the origin on all dimensions for independent $\text{Normal}(0,1)$ variables independent $\text{Uniform}(-\sqrt{3}, \sqrt{3})$.

dimension	5	10	15	20
Normal	297	44	7	1
Uniform	128	8	1	0

number of observations out of 2,000 to be within a threshold of 1 of the origin on all dimensions for Normal and Uniform data. This corresponds to the expected number of visible observations in a section using the default threshold of 1. Clearly for $p \geq 15$, sections have few observations, and the situation worsens moving away from the origin.

5.3 Touring algorithms

Real data is more clumpy than the Normal and Uniform samples summarised above, so we hope to find areas where the data lives and visualize these. Alternatively, we can look for interesting sections exhibiting features such as lack of fit, differences between fits, curvature or interaction. Some of the ideas presented in this section here were proposed in chapter 5 of the unpublished PhD dissertation of Mark O’Connell (O’Connell, 2017).

5.3.1 Visiting regions with data

The simplest strategy to find where the data lives is to pick random observations and use their coordinates for the conditioning predictors as sections points. We call this the `randomPath` tour,

and the user controls the number of random observations or path length with a slider. Other touring options form clusters in the conditioning observations. It is important to note that we are not trying to identify actual clusters in the data, rather to visit the parts of the predictor space where observations are located. We offer two tours based on clustering algorithms applied to the conditioning predictors C_{num}, C_{cat} : (i) `kmeansPath` which uses centroids of k-means clusters as sections and (ii) `kmedPath` which uses medoids of k-medoid clustering, available from the `pam` algorithm of package `cluster` (Maechler et al., 2019).

Both `kmeansPath` and `kmedPath` work for categorical as well as numerical variables. `kmeansPath` standardises numeric variables and hot-encodes categorical variables, `kmedPath` uses `daisy` from package `cluster` to form distances based on standardised Euclidean distances for a numeric dataset and Gower distance (Gower, 1971) for variables of mixed type. For our application we are not concerned with optimal clustering or choice of number of clusters, our goal is simply to visit regions where the data live. In our interactive implementation, the path length slider puts the number of clusters under user control.

For a broad comparison with Table 1, we calculate `randomPath`, `kmeansPath` and `kmedPath` tours of length 30 on datasets of 2,000 rows and 15 numeric variables obtained from the Ames (Cock, 2011) and Decathlon (Unwin, 2015) datasets. We also use simulated independent Normal and Uniform datasets of the same dimension. The results are summarised Table 2. In general, the

Table 2: Average number of visible observations in ($\sigma=1$) maxnorm slices at 30 section points and in parentheses their total similarity selected with `randomPath`, `kmeansPath` and `kmedPath` from Decathlon and Ames datasets and simulated Normal and Uniform datasets.

	random	kmeans	kmed
Decathlon	8.2 (1.8)	23.3 (3)	22.4 (3.7)
Ames	16.0 (4.3)	33.6 (8.4)	25.4 (7.6)
Normal	1.0 (1.0)	1.8 (0.2)	1.8 (1.1)
Uniform	1.1 (1.0)	0.9 (0.1)	1.3 (1.0)

number of observations visible in sections from real data far exceeds what might be expected based on calculations such as those in Table 1. Not surprisingly, paths based on both the clustering methods k-means and k-medoids find sections with many more observations than simply picking random observations.

We also show in Figure 7 the distribution of the maximum similarity per observation over

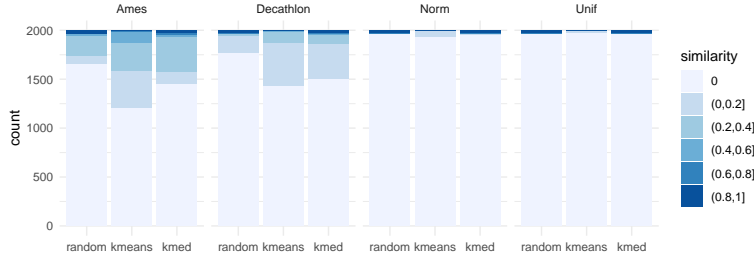


Figure 7: Distribution of the maximum similarity per observation across ($\sigma=1$) maxnorm slices at 30 section points selected with `randomPath`, `kmeansPath` and `kmedPath` from Decathlon and Ames datasets and simulated Normal and Uniform datasets.

the 30 section points for the three path algorithms and four datasets. In this example, paths based on clustering algorithms from both real datasets visit over 25% of the data. One advantage of k-medoids over k-means in this setting is that k-medoids used medoids that is, observations, rather than cluster centroids to define the section points, and these medoids will have similarity one.

5.3.2 Visiting regions exhibiting lack of fit

Other goals of touring algorithms might be to find regions where data is poorly fit, or where two or more fits give differing results. For numeric responses, the tour are called `lofPath` (for lack of fit) finds observations i whose value of

$$\max_{f \in \text{fits}} |y_i - \hat{y}_i^f|$$

is among the k (path length) largest, where \hat{y}_i^f is the prediction for observation i from fit f . For categorical responses, it finds observations where the predicted class does not match the observed class.

A fit are called `diffitsPath` (for difference of fit) finds observations i whose value of

$$\max_{f \neq f' \in \text{fits}} |\hat{y}_i^{f'} - \hat{y}_i^f|$$

is among the k (path length) largest for numeric fits. For fits to categorical responses, `diffitsPath` currently finds observations where there is the largest number of distinct predicted categories. In

future this could be adapted to use differences in prediction probabilities. Other paths could be constructed to identify sections with high amount of fit curvature or the presence of interaction.

5.3.3 Tours in `condvis2`

The tours presented here are a series of section plots $\hat{f}(\mathbf{x}_S = \mathbf{x}_{S^g}, \mathbf{x}_C = \mathbf{u}_C^k)$, showing slices formed around a series of section points $\{\mathbf{u}_C^k, k = 1, 2, \dots, l\}$. For each of the path algorithms, the section points are ordered using a seriation algorithm to form a short path through the section points—dendrogram seriation (Earle and Hurley, 2015) is used here, implemented using the package **DendSer** (Hurley and Earle, 2013).

Looking at a **condvis2** screenshot such as that in Figure 4, the tour controls are all in the lower left panel. Firstly, the tours listed in this section are available under the “Choose tour” menu, and “Tour length” controls the length of the computed path. The “Tour Step” slider controls the position along the current path; by clicking the arrow on the right the tour progresses automatically through the tour section points.

An interpolation option is available for smoothly changing paths, for this set the “Interp steps” slider to a positive number. Interpolation constructs a sequence of evenly spaced points between each pair of ordered section points. For quantitative predictors, this means linear interpolation, and for categorical predictors, we simply transition from one category to the next at the midpoints on the linear scale.

In the situation where some predictors designated as unimportant are relegated to F thus not appearing in the `condvis` display, the settings for predictors in F remain at their initial values throughout all tours. This means that section points for the tours based on selected observations (`randomPath`, `kmedPath`, `lofPath` and `diffitsPath`) will not in fact correspond exactly to dataset observations. An alternative strategy would be to let the settings for the predictors in F vary, but then there is a danger of being “lost in space”.

There are a few other simple tours that we have found useful in practice: tours that visit observations with high and low response values and tours that move along a selected condition variable, keeping other condition variables fixed at their current setting. It is also possible to pre-calculate a tour and feed it into the `condvis` function.

6 Case studies

We use the methodology of the previous sections to explore supervised learning fits in the regression and classification cases.

6.1 Bike sharing data

Here we use `condvis2` to explore predictor effects and goodness of fit for models fit to the bike sharing dataset, introduced in Section 3. To start with, we divide the data into training and testing sets using a 60/40 split. For the training data, we fit a linear model with no interaction terms, and a random forest which halves the RMSE by comparison with the linear fit. Comparing the two fits we see that the more flexible fit is better supported by the data, see for example Figure 8. In the fall, bike rentals are affected negatively by temperature according to the observed data. The linear fit does not pick up this trend, and even the random forest seems to underestimate the effect of temperature. Year is an important predictor: people used the bikes more in 2012 than in 2011. Switching the first section variable to wind, we would expect that the more wind the fewer people like to cycle, but the predicted number of bike rentals does not fall when wind speed increases from 25 to 35 km/h, but there is not much training data, so we suspect the random forest could not learn a meaningful prediction for this range.

We can also create a 2-d partial dependence plot (Figure 9) to see how the features interact: people cycle more when temperature is above 12C, but this effect depends on humidity.

By interacting with `condvis2` displays, we can see whether the joint effect of temperature and humidity changes with other features: comparing the fits in spring 2011, spring 2012 and fall 2012 we find that the joint effect of humidity and temperature changes through time; that is, we find a three-way interaction, see Figure 10. In these plots other conditioning variables were set to good weather/weekend/no holiday, but with further interactive exploration, we see that this effect is consistent at other levels.

Based on the information we have gleaned from our interactive exploration, an alternative parametric fit to the random forest might be a generalised additive model (gam) with a smooth joint term for temperature, humidity, an interaction between temperature and season, a smooth term for wind, and a linear term for remaining predictors. The gam fit has the additional advantage of providing confidence intervals, which could be added to the `condvis` display. Though



Figure 8: The random forest and linear model fit for the bike rentals training data.

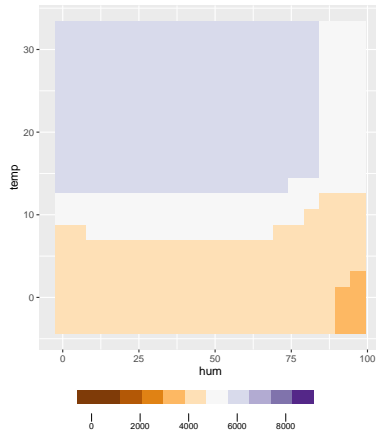
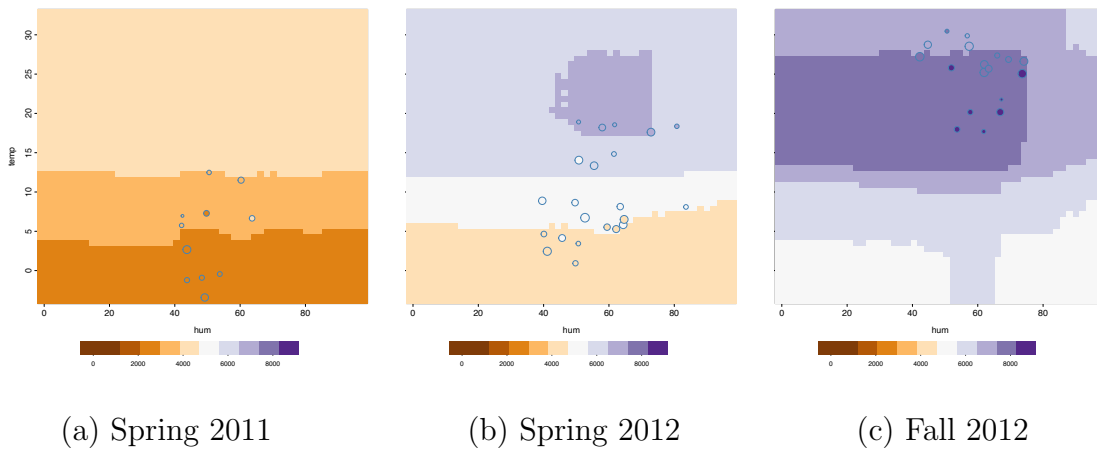


Figure 9: PDP plot for random forest fit to bike training data, showing effect of temperature and humidity on the predicted number of rentals. The plot combines the main effect of each of the features and their interaction effect.



(a) Spring 2011

(b) Spring 2012

(c) Fall 2012

Figure 10: Random forest fit to bike training data, with section predictors temperature and humidity, and the image colour shows the predicted number of rentals. In Spring 2011, temperature is the main driver of bike rentals, humidity has negligible impact. In Spring 2012 the number of bike rentals is higher than the previous year, especially at higher temperatures. In Fall 2012, bike rentals are higher than in spring, and high humidity reduces bike rentals. Other conditioning variables were set to good weather/weekend/no holiday.

the training RMSE for the random forest is considerably lower than that for the gam, on the test data the gam is a clear winner, see Table 3.

Table 3: Training and test RMSE for the random forest and gam fits to the bike data.

	RF	GAM
train	438.1	573.1
test	748.1	670.2

For a more detailed comparison of the two fits, we use condvis tours to move through various slices, here using the combined training and testing datasets. Figure 11 shows a k-medoid tour

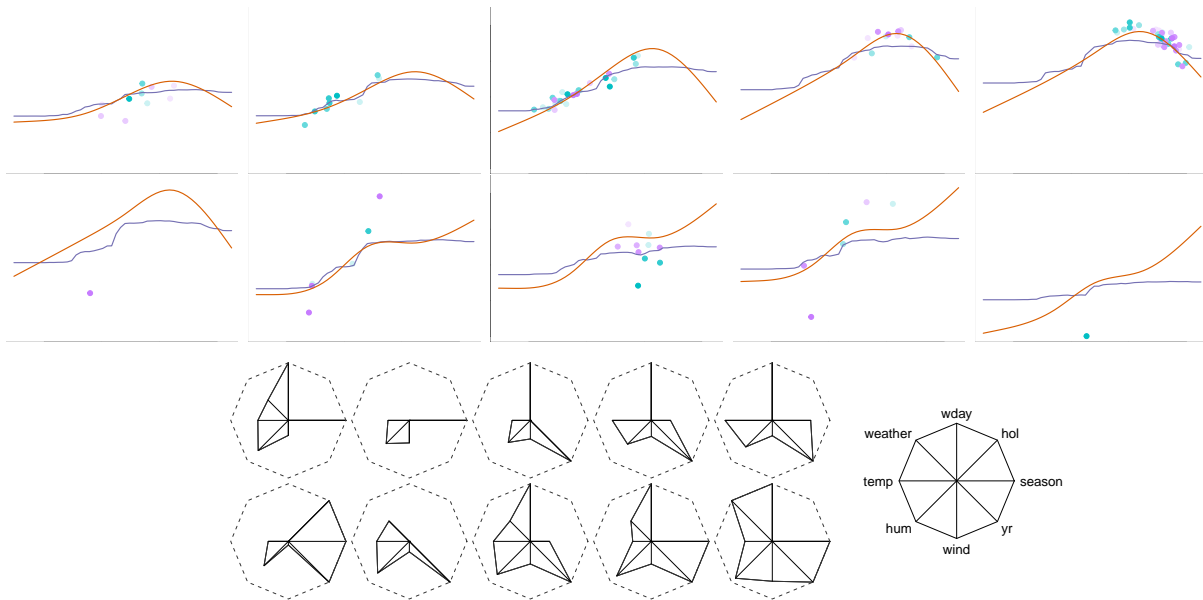


Figure 11: Condvis plots for showing tours of the bike data. Comparison of random forest fit in blue and gam in red, train and test observations are in light blue and pink respectively, rentals versus temperature. K-medoid tour in the first row, lack of fit tour in the second row. The stars show locations visited by the tours; k-medoid tour in the third row, and the lack of fit tour in the last row.

in the first row and lack of fit tour in the second row, with temp as the section variable and the remaining features forming the condition variables. (Here for purposes of illustration both tours are constructed to be of length 5). The last two rows of Figure 11 show the condition variable

settings for each of the ten tour points as stars, where a long (short) radial line-segment indicates a high (low) value for a condition variable. To the naked eye the gam fit looks to give better results for most of the locations visited by the k-medoid tour. Switching to the lack of fit tour, we see that the poorly-fit observation in each of the second row panels in Figure 11 has a large residual for both the random forest and the gam fits. Furthermore, the poorly-fit observations identified were all recorded in 2012, as is evident from the stars in the last row of Figure 11.

We can also construct `condvis` displays without showing any fit. One application of this is to compare predictions or residuals for an ensemble of model fits, as discussed in O’Connell (2017). For our current example we use a parallel coordinate plot to compare the response and predictions from the gam and random forest fits for the test data with the similarity threshold set so that the plot shows all summer, weekday, good weather days in 2012; see Figure 12. The gam predictions

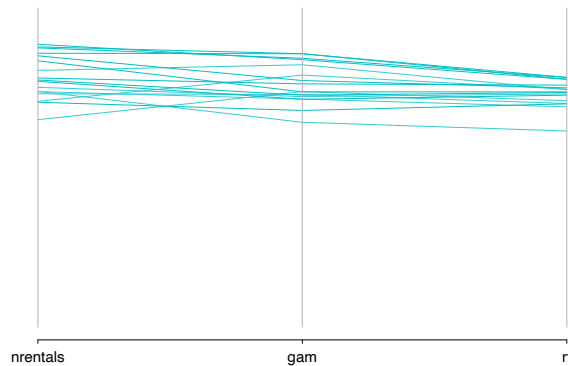


Figure 12: Paralell coordinate plot showing response and predictions from gam and random forest for summer, weekday, good weather days in 2012 from the bike test data.

are similar to the response as indicated by the mostly parallel line segment in the first panel, but the random forest underestimates the observed number of bike rentals. This pattern is not true for 2011 data.

6.2 Glaucoma data

Glaucoma is an eye disease caused by damage to the optic nerve, which can lead to blindness if left untreated. Early diagnosis is important, because with treatment, damage to eyesight can be arrested. In Kim et al. (2017), the authors explored various machine learning fits relating

the occurrence of glaucoma to age and various other features measured on the eye. The provided dataset comes pre-split into a training set of size 399 and a test set of size 100.

Here we use **condvis2** to compare a random forest and a C5.0 classification tree (Salzberg, 1994) fit to the training data. The random forest classified all training observations perfectly, mis-classifying two test set observations, whereas the tree misclassified 20 and 6 cases for the training and test data respectively. In a clinical setting however, as the authors in Kim et al. (2017) pointed out, the results from a classification tree are easier to understand and implement.

Figure 13 shows the training data with both classifiers. Here the section variables are PSD and

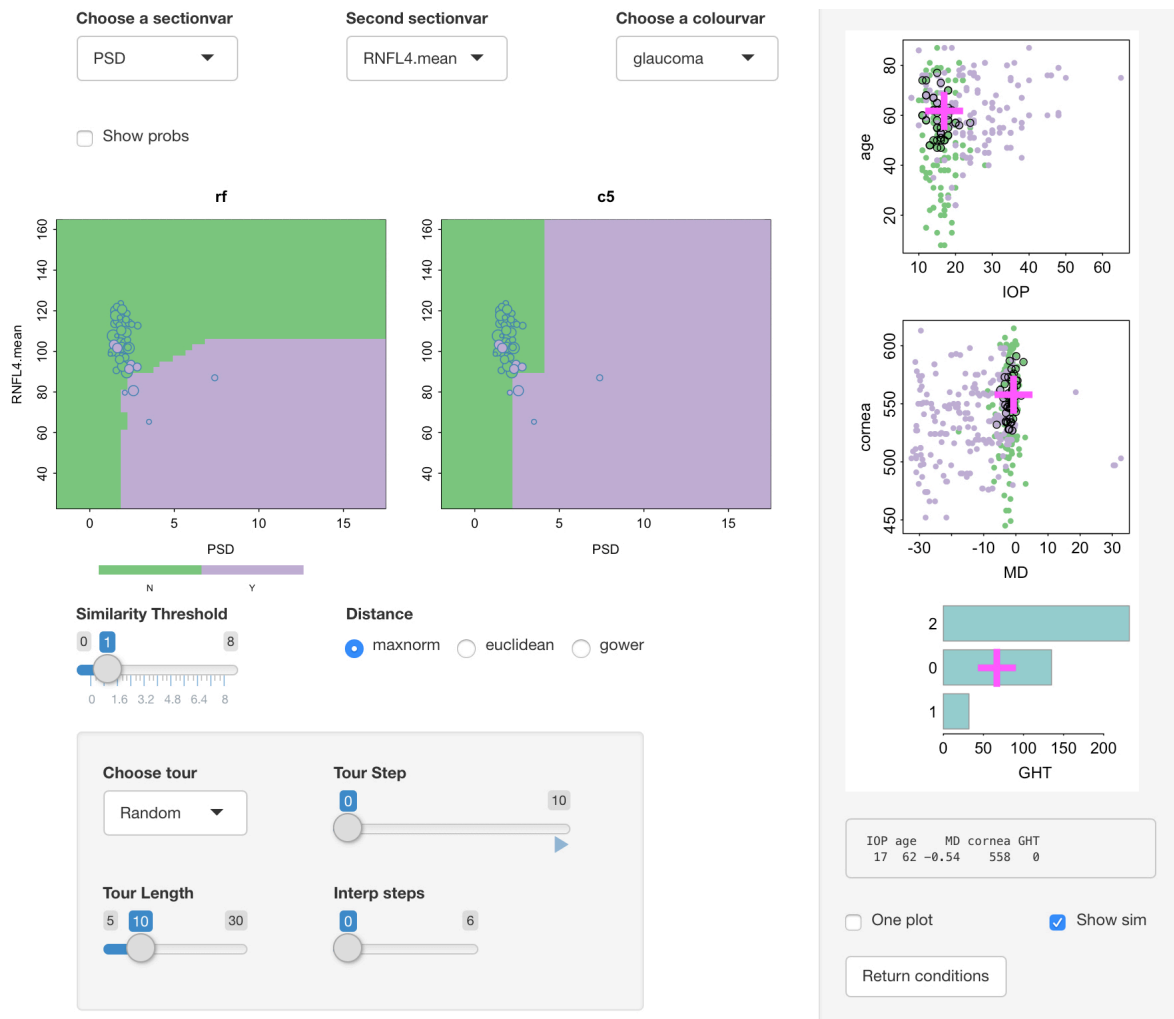
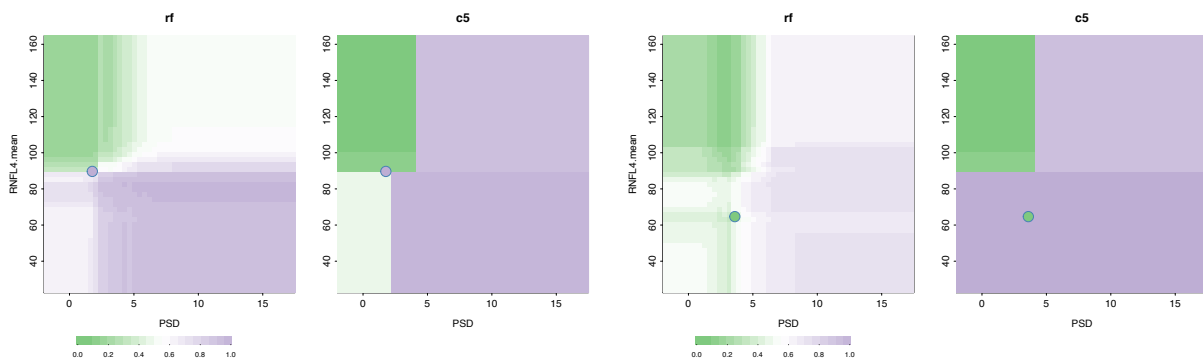


Figure 13: Random forest and tree fits for the Glaucoma training data. Cases drawn in purple have glaucoma.

RNFL.mean (the two most important features according to the random forest), and conditioning variables are set to values from the first case, who is glaucoma free. Both classifiers give similar results for this condition. Points whose colour in the section plots disagrees with the background colour of the classification surface are not necessarily mis-classified, they are just near (according to the similarity score) a region whose classification differs. Reducing the similarity threshold σ to zero would show points whose values on the conditioning predictors are identical to those of the first case, here just the first case itself, which is correctly classified by both classifiers. Clicking around on the condition selector plots and moving through the random, k-means and k-medoid tour paths shows that both classifiers give similar classification surfaces for section predictors PSD and RNFL.mean, in areas where observations live.

Using the lack of fit tour to explore where the C5 tree gives incorrect predictions, in Figure 14 the section plots show probability of glaucoma, on a green (for no glaucoma) to purple (for



(a) C5 false negative

(b) C5 false positive

Figure 14: Glaucoma training data, random forest and tree fits, surface shows probability of glaucoma. Cases drawn in purple have glaucoma. Panels show cases wrongly classified by the tree, a false negative in (a) and false positive in (b).

glaucoma) scale. In the left hand side panel figure 14(a) the C5 tree fit shows a false positive, which is quite close to the decision boundary. Though the random forest fit correctly classifies the observation, it does not do so with high probability. Figure 14(b) shows a situation where the tree gives a false positive. Here the similarity threshold σ is set to zero, so only the mis-classified observations are visible. Generally mis-classifications occur for low PSD values, and middling values of RNFL.mean, so for observations in this region, the tree fit may not be reliable.

7 Discussion

We have described a new, highly interactive application for deep-dive exploration of supervised and unsupervised learning model fits. This casts light on the black-box of machine learning algorithms, going far beyond simple numerical summaries such as mean squared error, accuracy and predictor importance measures. With interaction, the analyst can interrogate predictor effects and pickup higher-order interactions in a way not possible with partial dependence and ICE plots, explore goodness of fit to training or test datasets, and compare multiple fits. Our new methodology will help machine learning analysts, educators and students seeking to interpret, understand and explain model results. The application is currently useful for moderate sized datasets, up to 100,000 cases and 30 predictors in our experience. Beyond that, we recommend using case and predictor subsets to avoid lags in response time which make interactive use intolerable.

A previous paper (O’Connell et al., 2017) described the package **condvis**, the result of an early version of this project. Since then, in **condvis2** (available on CRAN) we have developed the project much further, and moved the implementation to a Shiny platform which supports a far superior level of interactivity. The choice of section plots and distance measures have been expanded. As an alternative to direct navigation through conditioning space, we provide various algorithms for constructing tours, designed to visit non-empty slices (**randomPath**, **kmeansPath** and **kmedPath**) or slices showing lack of fit (**lofPath**) or fit disparities (**diffitsPath**). We now offer an interface to a wide and extensible range of machine learning fits, through **CVpredict** methods, including clustering algorithms and density fits. By providing an interface to the popular **caret**, **parsnip**, **mlr** and **mlr3** model-building platforms our new interactive visualizations are widely accessible.

We recommend using variable importance measures to choose relevant section predictors, as in the case studies of Section 6. For pairs of section variables, feature interaction measures such as the H-statistic (Friedman and Popescu, 2008) could be used to identify interesting pairs for interactive exploration. New touring methods could be developed to uncover other section plot patterns, but this needs to be done in a computationally efficient way. A different approach to identifying interesting patterns could follow Cook (1995) who proposed reducing the dimension of the conditioning space using sufficient dimension reduction methods.

We note that the tours presented here are quite different to grand tours (Asimov, 1985), where the projection changes in small increments over time, and there is no slicing. In a recent paper (Laa et al., 2020), following on ideas from Furnas and Buja (1994), grand tours are combined

with slicing, where slices are formed in the space orthogonal to the current projection, but these techniques are not designed for the model fit setting.

There are some limitations in the specification of the section points through interaction with the condition selector plots, beyond the fact that large numbers of predictors will not fit in the space allocated to these plots (see Section 5.1). If a factor has a large number of levels, then space becomes an issue. One possibility is to display only the most frequent categories in the condition selector plots, gathering other categories into an “other” category, which of course is not selectable. Also, we have not as yet addressed the situation where predictors are nested.

Currently we offer a choice of three distance measures (Euclidean, maxnorm and Gower) driving the similarity weights used in section plot displays. Distances are calculated over predictors in C , other than those in F . Predictors are scaled to unit standard deviation before distance is calculated which may not be appropriate for highly skewed predictors, where a robust scaling is likely more suitable. We could also consider an option to interactively exclude some predictors from the distance calculation.

Other approaches could also be investigated for our section plot displays. Currently, the section plot shows the fit $\hat{f}(\mathbf{x}_S = \mathbf{x}_S^g, \mathbf{x}_C = \mathbf{u}_C)$ versus \mathbf{x}_S^g , overlaid on a subset of observations $(\mathbf{x}_{i,S}, y_i)$, where $\mathbf{x}_{i,C}$ belongs to the section around \mathbf{u}_C (assuming $F = \emptyset$). An alternative might be to display the average fit for observations in the section, that is

$$\text{ave}_{\mathbf{x}_{i,C} \in \text{sect}(\mathbf{u}_C)} \{ \hat{f}(\mathbf{x}_S = \mathbf{x}_S^g, \mathbf{x}_C = \mathbf{x}_{i,C}) \},$$

or, form a weighted average using the similarity weights. Such a version of a section plot is analogous to a local version of a partial dependence plot.

References

- Asimov, D., 1985. The grand tour: a tool for viewing multidimensional data. *Siam Journal on Scientific and Statistical Computing* 6, 128–143.
- Baniecki, H., Biecek, P., 2020. The grammar of interactive explanatory model analysis. CoRR abs/2005.00497.
URL <https://arxiv.org/abs/2005.00497>
- Becker, R. A., Cleveland, W. S., Shyu, M.-J., 1996. The visual design and control of trellis display.

- Journal of Computational and Graphical Statistics 5 (2), 123–155.
URL <https://amstat.tandfonline.com/doi/abs/10.1080/10618600.1996.10474701>
- Bellman, R., 1961. Adaptive Control Processes: A Guided Tour. Rand Corporation. Research studies. Princeton University Press.
URL <https://books.google.ie/books?id=POAmAAAAAAAJ>
- Bischl, B., Lang, M., Kotthoff, L., Schiffner, J., Richter, J., Studerus, E., Casalicchio, G., Jones, Z. M., 2016. mlr: Machine learning in r. Journal of Machine Learning Research 17 (170), 1–5.
URL <http://jmlr.org/papers/v17/15-066.html>
- Breiman, L., 2001. Random forests. Machine Learning 45 (1), 5–32.
URL <https://doi.org/10.1023/A:1010933404324>
- Britton, M., 2019. Vine: Visualizing statistical interactions in black box models. arXiv 1904.00561.
- Chambers, J., Cleveland, W., Kleiner, B., Tukey, P., 1983. Graphical Methods for Data Analysis. Wadsworth, Belmont, CA.
- Chang, W., Cheng, J., Allaire, J., Xie, Y., McPherson, J., 2020. Shiny: Web Application Framework for R. R package version 1.5.0.
URL <https://CRAN.R-project.org/package=shiny>
- Cock, D. D., 2011. Ames, iowa: Alternative to the boston housing data as an end of semester regression project. Journal of Statistics Education 19 (3), null.
URL <https://doi.org/10.1080/10691898.2011.11889627>
- Cook, D., Swayne, D. F., 2007. Interactive and Dynamic Graphics for Data Analysis With R and GGobi, 1st Edition. Springer Publishing Company, Incorporated.
- Cook, R. D., 1995. Graphics for studying net effects of regression predictors. Statistica Sinica 5 (2), 689–708.
URL <http://www.jstor.org/stable/24305064>
- Earle, D., Hurley, C. B., 2015. Advances in dendrogram seriation for application to visualization. Journal of Computational and Graphical Statistics 24 (1), 1–25.
URL <http://dx.doi.org/10.1080/10618600.2013.874295>

- Fanaee-T, H., Gama, J., 2013. Event labeling combining ensemble detectors and background knowledge. *Progress in Artificial Intelligence*, 1–15.
URL [\[WebLink\]](#)
- Flury, B., 1988. *Multivariate Statistics: A Practical Approach*. Chapman and Hall, Ltd., GBR.
- Friedman, J. H., 2001. Greedy function approximation: A gradient boosting machine. *The Annals of Statistics* 29 (5), 1189–1232.
URL <http://www.jstor.org/stable/2699986>
- Friedman, J. H., Popescu, B. E., 09 2008. Predictive learning via rule ensembles. *Ann. Appl. Stat.* 2 (3), 916–954.
URL <https://doi.org/10.1214/07-AOAS148>
- Furnas, G. W., Buja, A., 1994. Prosection views: Dimensional inference through sections and projections. *Journal of Computational and Graphical Statistics* 3 (4), 323–353.
URL <https://www.tandfonline.com/doi/abs/10.1080/10618600.1994.10474649>
- Goldstein, A., Kapelner, A., Bleich, J., Pitkin, E., 2015. Peeking inside the black box: Visualizing statistical learning with plots of individual conditional expectation. *Journal of Computational and Graphical Statistics* 24 (1), 44–65.
- Gower, J. C., 1971. A general coefficient of similarity and some of its properties. *Biometrics* 27 (4), 857–871.
URL <http://www.jstor.org/stable/2528823>
- Hastie, T., Tibshirani, R., Friedman, J., 2009. *The Elements of Statistical Learning: Data Mining, Inference, and Prediction*. Springer series in statistics. Springer.
URL <https://books.google.ie/books?id=eBSgoAEACAAJ>
- Hurley, C., O’Connell, M., Domijan, K., 2019. *Condivis2: Conditional Visualization for supervised and unsupervised models in Shiny*. R package version 0.1.1.
URL <https://CRAN.R-project.org/package=condivis>
- Hurley, C. B., 2020. Model exploration using conditional visualization. *Wiley Interdisciplinary Reviews: Computational Statistics*, in press.

- Hurley, C. B., Earle, D., 2013. DendSer: Dendrogram seriation: ordering for visualisation. R package version 1.0.1.
URL <http://CRAN.R-project.org/package=DendSer>
- Kim, S., J., C. K., Oh, S., 2017. Development of machine learning models for diagnosis of glaucoma. PLoS ONE 5 (e0177726).
- Kuhn, M., 2019. caret: Classification and Regression Training. R package version 6.0-84.
URL <https://CRAN.R-project.org/package=caret>
- Kuhn, M., Vaughan, D., 2019. parsnip: A Common API to Modeling and Analysis Functions. R package version 0.0.2.
URL <https://CRAN.R-project.org/package=parsnip>
- Laa, U., Cook, D., Valencia, G., 2020. A slice tour for finding hollowness in high-dimensional data. Journal of Computational and Graphical Statistics 29 (3), 681–687.
URL <https://doi.org/10.1080/10618600.2020.1777140>
- Lundberg, S. M., Lee, S.-I., 2017. A unified approach to interpreting model predictions. In: Guyon, I., Luxburg, U. V., Bengio, S., Wallach, H., Fergus, R., Vishwanathan, S., Garnett, R. (Eds.), Advances in Neural Information Processing Systems 30. Curran Associates, Inc., pp. 4765–4774.
URL <http://papers.nips.cc/paper/7062-a-unified-approach-to-interpreting-model-predictions.pdf>
- Maechler, M., Rousseeuw, P., Struyf, A., Hubert, M., Hornik, K., 2019. cluster: Cluster Analysis Basics and Extensions. R package version 2.1.0.
URL <https://CRAN.R-project.org/package=cluster>
- Martin, A. R., Ward, M. O., 1995. High dimensional brushing for interactive exploration of multivariate data. In: Proceedings Visualization '95. pp. 271–278.
- O'Connell, M., 2017. Conditional visualisation for statistical models. Ph.D. thesis, National University of Ireland Maynooth.
URL <http://mural.maynoothuniversity.ie/8141/>

- O’Connell, M., Hurley, C., Domijan, K., 2016. *Condvis: Conditional Visualization for Statistical Models*. R package version 0.1.1.
URL <https://CRAN.R-project.org/package=condvis>
- O’Connell, M., Hurley, C., Domijan, K., 2017. Conditional visualization for statistical models: An introduction to the condvis package in R. *Journal of Statistical Software, Articles* 81 (5), 1–20.
URL <https://www.jstatsoft.org/v081/i05>
- Ribeiro, M. T., Singh, S., Guestrin, C., 2016. “Why should I trust you?”: Explaining the predictions of any classifier. In: *Proceedings of the 22nd ACM SIGKDD International Conference on Knowledge Discovery and Data Mining, San Francisco, CA, USA, August 13-17, 2016*. pp. 1135–1144.
- Salzberg, S. L., 1994. *C4.5: Programs for machine learning by j. ross quinlan*. morgan kaufmann publishers, inc., 1993. *Machine Learning* 16 (3), 235–240.
URL <https://doi.org/10.1007/BF00993309>
- Scott, D. W., 2015. *Multivariate Density Estimation: Theory, Practice, and Visualization*. Wiley Series in Probability and Statistics. Wiley.
- Scrucca, L., Fop, M., Murphy, T. B., Raftery, A. E., 2016. mclust 5: clustering, classification and density estimation using Gaussian finite mixture models. *The R Journal* 8 (1), 289–317.
URL <https://doi.org/10.32614/RJ-2016-021>
- Staniak, M., Biecek, P., 2018. Explanations of Model Predictions with live and breakDown Packages. *The R Journal* 10 (2), 395–409.
URL <https://doi.org/10.32614/RJ-2018-072>
- Stuetzle, W., 1987. Plot windows. *Journal of the American Statistical Association* 82 (398), 466–475.
URL <http://www.jstor.org/stable/2289448>
- Tufte, E. R., 1986. *The Visual Display of Quantitative Information*. Graphics Press, Cheshire, CT, USA.

Unwin, A., 2015. GDadata: Datasets for the Book Graphical Data Analysis with R. R package version 0.93.

URL <https://CRAN.R-project.org/package=GDadata>

Urbanek, S., 2002. Different ways to see a tree - klimt. In: Härdle, W., Rönz, B. (Eds.), *Compstat. Physica-Verlag HD, Heidelberg*, pp. 303–308.

Waddell, A., Oldford, R. W., 2020. loon: Interactive Statistical Data Visualization. R package version 1.3.1.

URL <https://CRAN.R-project.org/package=loon>

Wickham, H., 2016. *ggplot2: Elegant Graphics for Data Analysis*. Springer-Verlag New York.

URL <https://ggplot2.tidyverse.org>

Wilkinson, L., 2005. *The Grammar of Graphics (Statistics and Computing)*. Springer-Verlag New York, Inc., Secaucus, NJ, USA.